Autoencoder-based Ultrasonic NDT of Adhesive Bonds

Ivan Kraljevski
Cognitive Material Diagnostics
Fraunhofer IKTS
Cottbus, Germany
ivan.kraljevski@ikts.fraunhofer.de

Frank Duckhorn
Machine Learning and Data Analysis
Fraunhofer IKTS
Dresden, Germany
frank.duckhorn@ikts.fraunhofer.de

Martin Barth
Ultrasonic Sensors and Methods
Fraunhofer IKTS
Dresden, Germany
martin.barth@ikts.fraunhofer.de

Constanze Tschoepe
Machine Learning and Data Analysis
Fraunhofer IKTS
Dresden, Germany
constanze.tschoepe@ikts.fraunhofer.de

Frank Schubert
Ultrasonic Sensors and Methods
Fraunhofer IKTS
Dresden, Germany
frank.schubert@ikts.fraunhofer.de

Matthias Wolff
Chair of Communications Engineering
BTU Cottbus-Senftenberg
Cottbus, Germany
matthias.wolff@b-tu.de

***Abstract*—We present an approach for ultrasonic non-destructive testing of adhesive bonding employing unsupervised machine learning with autoencoders.**

The models are trained exclusively on the features derived from pulse-echo ultrasonic signals on a specimen with good adhesive bonding and tested on another specimen with artificially added defects.

The resulting pseudo-probabilities indicating anomalies are visualized and presented along to the C-scan of the same specimen. As a result, we achieved improved representation of the defects, allowing their automatic and reliable detection.

I. Introduction

Adhesive bonding is one of the oldest manufacturing and repair processes where components are bonded surface-to-surface using adhesives. Modern adhesives are indispensable in many industries and application areas, such as automotive, aerospace and marine industry, electronics and telecommunications, medical devices, household appliances, furniture manufacturing, and many others. Adhesive bonding as a joining technique has many advantages, such as homogeneous load distribution, electrolytic and corrosion protection, long service lifetime, design of complex structures, sealing properties, and a possibility to join dissimilar materials [1].

On the other hand, the disadvantages are mainly related to the joining process itself (surface preparation, mixing, curing) and the limitations in the service due to the temperature and environmental factors that introduce changing properties of the bonding over its lifetime [2]. The adhesive bonds are prone to defects, which can occur during the joining process or later in service due to fatigue and usage. The defects can appear in the form of cracks, weak bonds and adhesive layers, disbonds and voids (most prevalent [3]), porosity, and contamination [4].

Parts of the study have been supported by the Ministry of Science, Research and Culture of Brandenburg (project "Kognitive Materialdiagnostik", grant #22-F241-03-FhG/007/001) and by the German Federal Ministry for Economic Affairs and Energy (ZIM project "KlassUS", grant KF 2455306WM3).

Evaluation of the quality of adhesive joints employing non-destructive testing (NDT) methods is challenging because they usually vary significantly in size, shape, and thickness, even in the same specimen. The ultrasonic and vibrations methods are the most common conventional NDT approaches for inspecting adhesive bonds [5]. They rely on mechanical waves, where the features of the response (echo) signal such as the frequency, envelope (form), the amplitude are critical parameters for assessing the adhesive bond quality [6].

They are categorized into three groups [7]: first, the pulse-echo and through-transmission techniques are utilized for detecting voids and disbonds. The second, acoustic resonance-based and ultrasonic resonance spectroscopy methods have been proposed to evaluate layered structures [3]. The third group includes guided waves ultrasound techniques predominantly used for bond detection and sizing but are also suited for bond strength evaluation.

Whichever method is employed, the adhesive bonding testing usually involves extensive post-processing and tuning, such as denoising, signals alignment, surface reflections removal, and finding the proper time window of interest. In the end, the signals are visualized as two-dimensional images of the adhesive-bonded specimens [8]. In most cases, a trained expert primarily sets the analysis parameters and interprets ultrasonic scans. However, more advanced signal analysis and machine learning algorithms can simplify the procedure, improve the visualizations and enable automatic defect detection.

This paper presents a methodology for ultrasonic NDT of adhesive bonds using an unsupervised machine learning approach with autoencoders (AE). The AE is trained exclusively on pulse-echo signals recorded on an object consisting of aluminum sheets with appropriate adhesive bonding.
The trained model is used for inference on another specimen with artificial defects. The results are visualized as two-dimensional matrices of spatially distributed pseudo-probabilities indicating normal or anomalous bonding.

TABLE I
SPECIMENS (ALUMINUM, 4 X 2 MM, 310 MM X 150 MM)

specimen	set	samples	defects
p31v	training	4416	none
p31v	validation	1104	none
p32v	test	11856	cavity, adhesive strips

II. MATERIAL AND METHODS

A. Data Collection and Organization

The two specimens (Table I) used in the experiments are constructed by adhesive bonding (3M DP760) of four AlMg3 sheets with 2 mm thickness each. Specimen *p31v* has no defects, where the *p32v* contains artificially introduced defects of different types: cavity and adhesive strips.

Fig. 1 presents a reference through-transmission C-Scan obtained in a scanning acoustic microscope using two focused ultrasound transducers with center frequencies of about 20 MHz. The artificially introduced defects emulate complete voids (cavity) and foreign bodies (adhesive strips) and are entirely distinguishable. Additionally, there are unintentional defects at the object's edges as a result of imperfect bonding (as on the right edge of the object in Fig. 1).

The objective is to perform NDT using an ultrasonic probe on an object from one side only. Hence, pulse-echo measurements were conducted using a 5 MHz ultrasonic transducer yielding signals with a sample rate of 25 MS/s. Each specimen was scanned over both axes, the 310 mm and 150 mm, with a 2 mm stride, providing 11856 signals per specimen, annotated with their position on the 156 x 76 grid.

B. Feature Analysis

As features, we use the raw transducer readings (SIG) as analog signals A/D converted in the big-endian PCM format and 16-bit resolution. A duration of 20 μs and a sample rate of 25 MS/s give feature samples of a dimension of 500×1.

The signals are re-aligned by a trigger that finds the positive amplitude onset greater than a preset threshold (10% full scale). That ensured consistency across the signal onsets, compensating the distance variations between the ultrasonic transducer and the measured object.

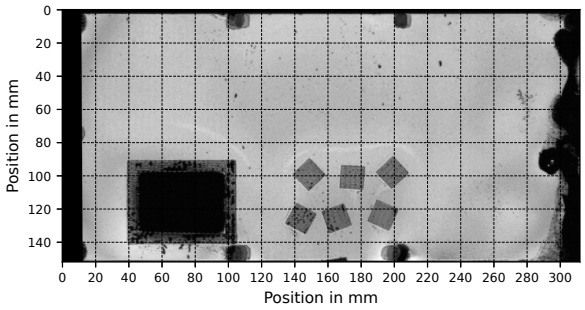

Fig. 1. Reference through-transmission C-Scan of the p32v.

There are variations in the thickness of the bonding layers across the objects and unwanted reflections from the object edges. In order to compensate for these effects, additional feature analysis (PFA) using the raw signals were performed. The PFA features were created by calculating the log magnitude spectrum with a Blackman window with a length of 75, yielding features with a dimension of 86×16 per grid point.

III. EXPERIMENT SETUP

To perform NDT utilizing anomaly detection, we employed autoencoders (AE), deep neural networks whose architecture consists of two parts: an encoder that transforms the input to a compressed representation and a decoder which approximately reconstructs the input data as well as possible according to the learned representation (under-complete autoencoder) [9]. Bottleneck hidden layer(s) force(s) the network to learn the data's salient features and prevents the input data from simply passing to the output.

The AE models were trained on the ultrasonic signals using the Keras [10], and Tensorflow [11], to reconstruct the input samples by minimizing the mean-squared error (MSE) as the loss function. If an anomalous sample is tested, the trained autoencoder will fail to reconstruct it successfully, producing a higher than expected MSE.

The MSE is considered to be a deviation score from the "normal state" and $MSE(x) \in [0, \infty)$, which were transformed into a pseudo posterior probability $P(c_1|x) \in [0, 1]$ of the sample x belonging to the "normal" state's class c_1. A sample is considered anomalous (class c_0) if this pseudo-probability falls below an estimated threshold [12].

Pseudo-probabilities are estimated by applying a sigmoid function of the MSE of a sample x of the test dataset $\mathcal{D}_{test}$:

$$P(c_1|x) = \frac{1}{1 + \mathrm{e}^{-MSE(x)}}, \quad x \in \mathcal{D}_{test}. \tag{1}$$

We performed a grid search over the initial network architecture with three hidden fully connected layers to estimate optimal network layout and parameters and vary the number of neurons in the layers. The number of units in the bottleneck layer was kept smaller than the preceding and the following ones. The optimal setup was determined in 10 training epochs by the loss on the validation set (pre-selected 20% of the training samples).

The optimal architecture consists of three hidden layers with 250, 150, and 250 neurons, correspondingly. Both encoder and decoder layers use hyperbolic tangent activation (tanh) function and RMSprop [13] as gradient-based optimizer.

To avoid over-fitting on such a network with relatively small capacity, we used early stopping with the criteria of 5 epochs without an improvement in the loss on the validation set (20%). The training and validation set were selected (in total, 5520 samples) from the central region of the specimen *p31v* where the adhesive bonding was successful and most consistent.

TABLE II
PERCENT OF OUTLIERS WITH 95% CONFIDENCE INTERVALS

SIG	PFA
$5.163^{+0.617}_{-0.569}$	$3.424^{+0.514}_{-0.464}$

IV. RESULTS AND DISCUSSION

First, we investigated the quality of the AE models for each feature type (SIG and PFA). We estimated the percent of training samples with MSE values outside a threshold θ determined by the interquartile range rule (Q1 is the first and Q3 the third quartile):

$$\theta = Q1 - 1.5 \cdot IQR, \text{ where } IQR = Q3 - Q1. \quad (2)$$

Table II presents the percent of samples of the training set ($p31v$), which would be considered as outliers according to the IQR-based threshold. That indicates inconsistencies in the training set related to variable bonding thickness. The PFA features, as more consistent, yielded fewer outliers than the SIG features.

Since the trained models are tested on another specimen with different physical properties and measurement conditions, it would be inappropriate to use the threshold θ estimated only on the training specimen for defects detection.

The resulting pseudo-probabilities are inferred from the model created on the training specimen, therefore it is necessary to re-scale the pseudo-probabilities and recalculate the threshold for defect detection for another specimen. That can be done automatically by setting the threshold using standard statistical or clustering methods.

Fig. 2-a shows a normal pulse-echo C-scan (5 MHz transducer) where the maximum amplitude value of a certain time interval after the surface echo is re-scaled and color-coded. Usual post-processing includes a cut in time, focusing the time interval of interest, mainly after the first strong echo, and averaging over time with root-main-square (RMS) to reduce signal fluctuations. In comparison with the reference amplitude through-transmission C-scan (Fig. 1), the pulse-echo C-scan (Fig. 2-a) exhibits strong echos with less transmission and increased signal distortion due to multiple reflections.

Additionally, layers with varying thicknesses contribute to signal fluctuations. The adhesive layer echoes merge into each other, and some defects are not detectable, like the adhesive strips (marked with a red rectangle).

Fig. 2-b and 2-c present the visualizations of the pseudo-probabilities obtained with the AE trained on SIG (b) and PFA (c) features, where the brighter spectral colors (yellow and red) indicate a higher probability of an anomaly or defect. In contrast to the C-scan, both exhibit better representation of the defects, with high contrast against areas with proper bonding. That enables any prospective defect detection or even type classification procedure feasible.

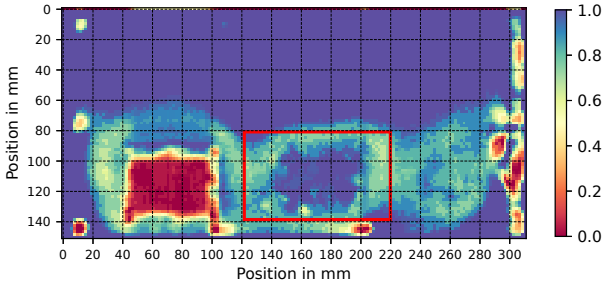

(a) 5 MHz pulse-echo ultrasonic C-scan.

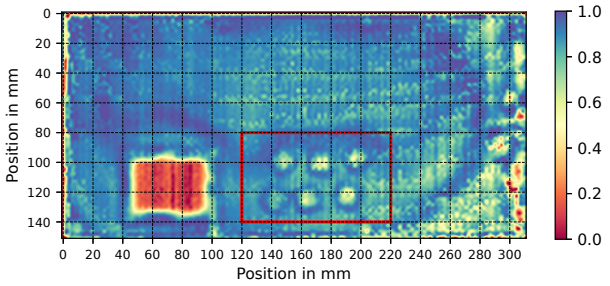

(b) Pseudo-probabilities with SIG features.

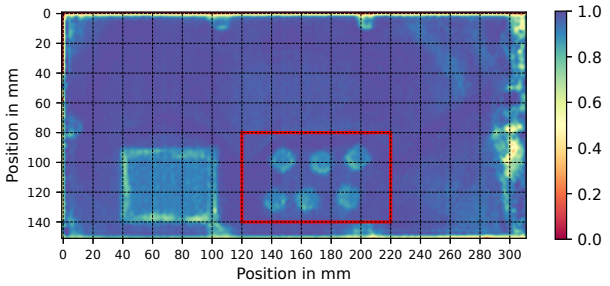

(c) Pseudo-probabilities with PFA features.

Fig. 2. C-scan and pseudo-probabilities for the test specimen p32v.

V. CONCLUSION

We investigated ultrasonic NDT with autoencoders trained on pulse-echo signals to detect and visualize defects in adhesive bonding. The models are trained on signals from only one specimen with good adhesive bonding and tested on signals of a specimen with incorporated defects.

The process is entirely automatic and reproducible on other specimens once the autoencoder model is trained. The pseudo-probabilities have absolute values between 0 and 1, which are easily interpretable and suitable for anomaly detection using a calculated threshold for decision.

There is no need for intervention by a human expert for setting analysis parameters, which is considered challenging due to signal fluctuations.

Future work will aim to not only to detect defects reliably but also to evaluate the bond strength of adhesive joints.

REFERENCES

[1] S. Budhe, M.D. Banea, S. de Barros, and L.F.M. da Silva, "An updated review of adhesively bonded joints in composite materials," *International Journal of Adhesion and Adhesives*, vol. 72, pp. 30–42, 2017.

[2] Walter Brockmann, Paul Ludwig Geiß, Jürgen Klingen, and K Bernhard Schröder, *Adhesive bonding: materials, applications and technology*, John Wiley & Sons, 2008.

[3] Elena Maeva, Inna Severina, Sergiy Bondarenko, Gilbert Chapman, Brian O'Neill, Fedar Severin, and Roman Gr. Maev, "Acoustical methods for the investigation of adhesively bonded structures: A review," *Canadian Journal of Physics*, vol. 82, no. 12, pp. 981–1025, 2004.

[4] RD Adams and BW Drinkwater, "Nondestructive testing of adhesively-bonded joints," *NDT & E International*, vol. 30, no. 2, pp. 93–98, 1997.

[5] Lester W Schmerr, *Fundamentals of ultrasonic nondestructive evaluation*, Springer, 2016.

[6] Bastien Ehrhart, Bernd Valeske, Charles-Edouard Muller, and Clemens Bockenheimer, "Methods for the quality assessment of adhesive bonded CFRP structures-a resumé," in *2nd International Symposium on NDT in Aerospace*, 2010, vol. 2010.

[7] Mehdi Zeighami and Farhang Honarvar, "New approaches for testing of adhesive joints by ultrasonic C-scan imaging technique," *Materials evaluation*, vol. 67, no. 8, pp. 945–954, 2009.

[8] Bengisu Yılmaz and Elena Jasiūnienė, "Advanced ultrasonic NDT for weak bond detection in composite-adhesive bonded structures," *International Journal of Adhesion and Adhesives*, vol. 102, pp. 102675, 2020.

[9] Ian Goodfellow, Yoshua Bengio, and Aaron Courville, *Deep Learning*, MIT Press, 2016.

[10] François Chollet et al., "Keras," https://keras.io, 2015.

[11] M. Martín et al., "Tensorflow: A system for large-scale machine learning," in *12th USENIX Symposium on Operating Systems Design and Implementation (OSDI 16)*, 2016, pp. 265–283.

[12] Ivan Kraljevski, Frank Duckhorn, Constanze Tschöpe, and Matthias Wolff, "Machine Learning for Anomaly Assessment in Sensor Networks for NDT in Aerospace," *IEEE Sensors Journal*, vol. 21, no. 9, pp. 11000–11008, 2021.

[13] Tijmen Tieleman and Geoffrey Hinton, "Lecture 6.5-rmsprop: Divide the gradient by a running average of its recent magnitude," *COURSERA: Neural networks for machine learning*, vol. 4, no. 2, pp. 26–31, 2012.